



Semester Project
Advanced NEMS Laboratory
École Polytechnique Fédérale de Lausanne

Study of HfO₂ Crystallization Using Annealing and X-ray Diffraction

Bruder, Andrea Alessandro

Under the direction of
Prof. Luis Guillermo VILLANUEVA
and supervisor
Ph.D. Daniel MORENO

Spring 2022

Table of content

1	Introduction	3
2	Microfabrication of HfO₂ chips	4
2.1	Photolithography (sideproject)	4
2.2	Descume	6
2.3	Evaporation	6
2.4	Atomic Layer Deposition (ALD)	7
2.5	Lift-Off	9
2.6	Stress Measurement	9
2.7	Fence Height Measurement (sideproject)	10
2.8	Thickness Measurement	11
3	HfO₂ Crystallization	14
3.1	Crystallinity	14
3.2	Annealing	14
3.3	X-Ray Diffractometry	15
3.4	Results	15
3.5	Discussion	17
4	Conclusion	18
	References	19
A	Process Flow	21
B	Stress Measurements	26
C	Thickness Measurements	28
D	XRD 2θ Measurements	30

List of Figures

1	Process flow summary	4
2	Pattern destruction by comet.	5
3	Schematic representation of maskless exposure through a spatial light modulator.	5
4	Schematic representation of photolithography process.	6
5	Schematic representation of 2 photoresists with undercut after double development.	6
6	Schematic representation of divided plasma chamber with radical species etching.	7
7	Schematic representation an E-Beam evaporator.	8
8	Schematic representation of an atomic layer deposition cycle	8
9	Schematic representation of etching vs. lift-off.	9
10	Schematic representation of stress measurement.	10
11	Surface topology and (non-existing) fences.	10
12	LR wafer: Stress and curvature measurements over 2 directions.	12
13	LR Wafer: Thickness measurements after 2 (left) and 3 (right) deposits.	13
14	HfO ₂ crystal structures, from left to right: Tetragonal, Orthorhombic I, Monoclinic.	14
15	LR wafer: 2θ measurements after annealing.	16
16	Process flow (including sideproject).	25
17	HR wafer: Stress and curvature measurements over 2 directions.	26
18	LR wafer with SiO ₂ : Stress and curvature measurements over 2 directions.	27
19	HR wafer: Thickness measurements after 1 (left), 2 (middle) and 3 (right) deposits.	28
20	LR with SiO ₂ layer wafer: Thickness measurements after 1 (left), 2 (middle) and 3 (right) deposits.	29
21	HR wafer (HR): 2θ measurements after annealing.	30
22	LR wafer with SiO ₂ layer (S): 2θ measurements after annealing.	31

1 Introduction

Due to its chemical properties, hafnium oxide (HfO₂) has been receiving more and more attention for a variety of applications. Nonetheless, a main concern remains the incertitude of how to achieve one of the 3 different crystal states (monoclinic, tetragonal or orthorhombic). Depending on the crystal structures, respectively the asymmetry/ symmetry of the atom allocation, the material can emit piezoelectric behavior under zero stress. Especially for cantilever based nanoactuators, which can consist of a thin film HfO₂ engaged between two platinum layers, it is desirable that the HfO₂ has perfect symmetry (monoclinic phase), respectively does not induce a polarisation in the ground state to facilitate frequency readout without offset.

Therefore the main goal of this project was to elaborate different annealing techniques to get monoclinic thin film HfO₂. The process done to manufacture the test samples is described in chapter 2 and comprises a HfO₂ deposition between two platinum layers on 3 different types of Si/ SiO₂ substrates. Then chapter 3 evaluates, based on X-ray diffraction, the results achieved after different annealing procedures. Even though no monoclinic phase has been attained with the given tools, the same chapter provides a detailed discussion of possible annealing improvements, such as higher maximum temperatures, etc. to attain the monoclinic phase in another trial.

Please note that parallel to the main project of evaluating annealing techniques for HfO₂, the manufacturing of the cantilever based oscillators has been started and is still to be continued. This was done for efficiency reasons, as it in general needs the same process steps, and for personal curiosity to explore more microfabrication procedures. The steps uniquely done for this project are marked as *sideproject* in the process flow and were as well done on the 3 different types of wafers.

2 Microfabrication of HfO₂ chips

This chapter provides an overview over the different microfabrication steps made at the Center of MicroNanotechnology (CMi) to manufacture the HfO₂ samples for further crystallization analysis. A summary of the procedure is given in figure 1, whereas the detailed process flow and the corresponding parameters can be found in appendix A. The process was done with 3 different types of 525 μm thick $\langle 100 \rangle$ silicon wafers, namely low resist (0.1 – 100 $\Omega\text{-cm}$), hard resist (> 10'000 $\Omega\text{-cm}$) and low resist (0.1 – 100 $\Omega\text{-cm}$) with a 2 μm thick SiO₂ surface layer for each of the 2 projects. All three substrates went through the same procedure to, among other things, compare the annealing behavior of HfO₂ on different substrate structures. The process started with a descum of the wafers (subsection: 2.2), followed by the first 20nm Cr/Pt thermal evaporation (2.3) and the 50nm HfO₂ atomic layer deposition (2.4) and ended with the second 20nm Cr/Pt evaporation. Parallel to the process several measurements for the internal stress (2.6) and the thickness (2.8) of the deposited materials were made. Additionally, the sideproject steps photolithography, lift-off and fence measurement are explained in subchapter 2.1, 2.5 and 2.7.

Summary Process Flow	
Main project (study of HfO ₂ crystallisation)	Sideproject (HfO ₂ based nanoactuators)
Stress Measurement	-
Descum	Descum
-	Photolithography
20nm Pt Evaporation	20nm Pt Evaporation
Stress Measurement	Lift Off
-	Fence Measurement
50nm HfO ₂ ALD	50nm HfO ₂ ALD
Stress Measurement	-
20nm Pt Evaporation	20nm Pt Evaporation
Stress Measurement	To continue (refer to detailed process flow)...
Thickness Measurement	
Dicing	
Annealing	

Figure 1: Process flow summary

2.1 Photolithography (sideproject)

Photolithography is a method to pattern something on a substrate by using (a mask and) a light sensitive photoresist. The process itself can be subdivided into three stages, namely: Coating, exposure and development (Cirelli & al, 2001).

The first step of the process is to uniformly deposit a photoresist on the substrate. This was done with the EVG 150, which can automatically do positive photoresist coating, development, softbake and post exposure bake on its three hot plates (CMI: Racine G.-A., 2020). Before the resist is deposited on the substrate, the wafer is heated up to 160°C to dehydrate its surface and to ensure a proper attachment of the resist layer. Next, the two photoresist layers LOR5A (thickness: 0.48 μm) and AZ1512 (thickness: 1.1 μm) are

one after the other automatically deposited by spin coating and softbaked to harden. If the machine, i.e. the resist dispenser, contains (dried) resist particles, which are as well deposited on the wafer, comets can appear and destroy parts of latter drawn pattern such as in figure 2.

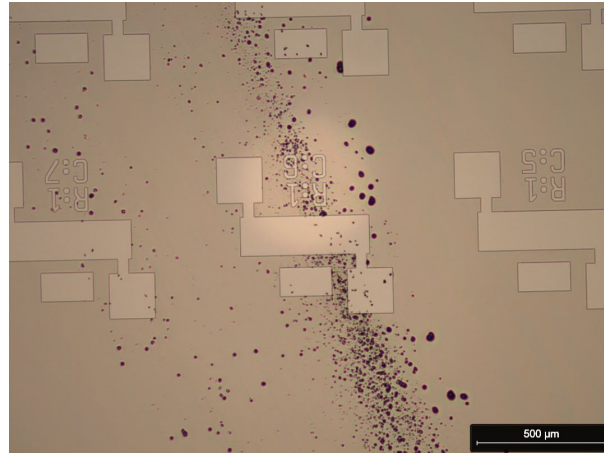


Figure 2: Pattern destruction by comet.

In the next step of the photolithography process the resist on the wafer is exposed to light at certain locations, which alters the chemical bonding of the photoresist. Depending on a positive or negative type photoresist, the bonds between the atoms get reinforced or weakened. The CAD pattern itself, respectively the light-exposed area is either defined by a photomask or trough a spatial light modulator, which does not enlighten the whole wafer area, but goes pixel per pixel over the wafer to expose only the desired surface points (figure 3). Former is in general used in industrial processes for high volume manufacturing as it requires a time-consuming production of the mask, while later is more suitable for R&D projects, which have small volumes and require constant redesigns of the pattern (Heidelberg, 2022). Therefore, the MLA150 from Heidelberg Instruments was used for this project, which scanned the resist with the $\lambda = 405\text{nm}$ laser source at a focal distance of $-2\mu\text{m}$ and an intensity of $55\text{mJ}/\text{cm}^2$.

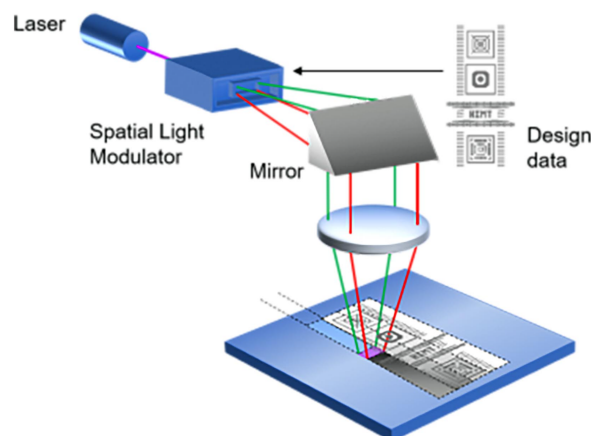


Figure 3: Schematic representation of maskless exposure through a spatial light modulator. (Heidelberg, 2022)

After the exposure, either the exposed or unexposed photoresist gets developed to create a topological mask such as in figure 4. With LOR5A and AZ1512, both positive resists, the UV light exposed regions disappear and the wafer with the remaining resist is then post-exposure baked to solidify the remaining resist for further etching processes. It is important to note that the development process was done twice. Using a photoresist bilayer and doing double development creates undercuts (figure 5), which minimize the risk of having fences at the lateral walls from the thermal evaporation process (2.3), which could later induce short circuits between the 2 platinum layers.

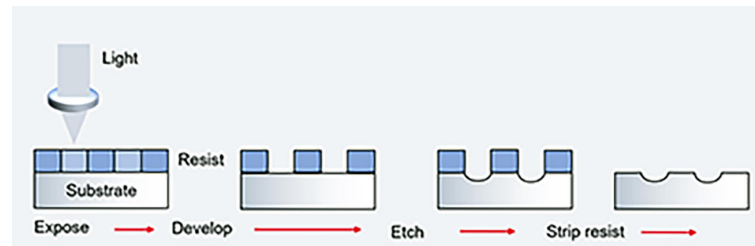


Figure 4: Schematic representation of photolithography process. (Heidelberg, 2022)

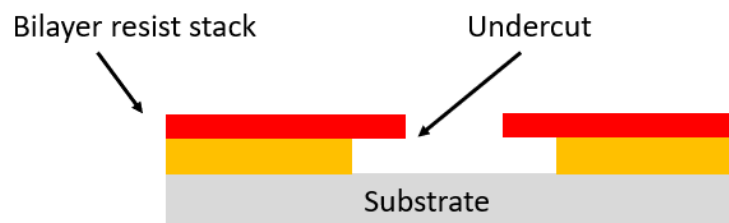


Figure 5: Schematic representation of 2 photoresists with undercut after double development.

2.2 Descume

Descume, a way of plasma ashing, is used to remove photoresist residues and to pursue wafer surface cleaning (PIC, -). The ions and radical (oxygen) species generated in the mostly oxygen plasma either bombard the sample physically or oxidize with the photoresist by generating high vapor pressure by-products such as CO, CO₂ or H₂O (Samco, -). However, bombardment does not only etch desired areas, but also causes damage to and charging of the substrate. A solution to this issue is to separate the plasma from the sample by placing the grounded electrode above the sample, such that only radical species are used to chemically react with the residues and no ion bombardment happens. A schematic description of this setup for the used Tepla GiGAbatch can be found in figure 6. All samples were exposed to the plasma for 30s at low power (200W) (CMi, 2019).

2.3 Evaporation

The thermal evaporation process is a physical vapor deposition method to coat thin films on substrates. The main concept can be seen in figure 7 and includes sputtering

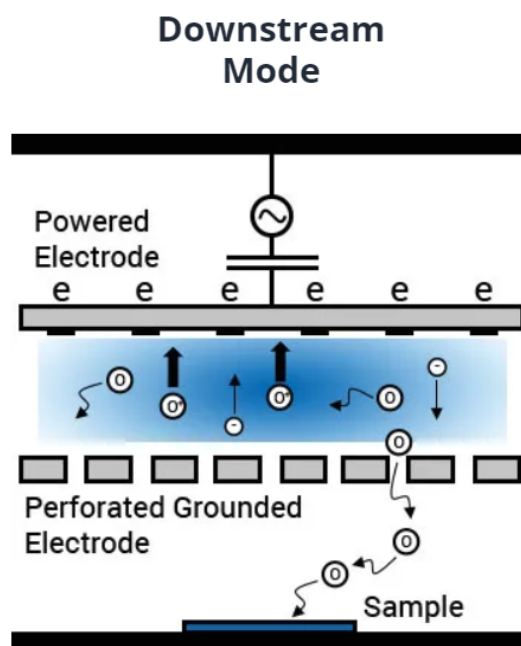


Figure 6: Schematic representation of divided plasma chamber with radical species etching.
(Samco, -)

away a source material, which traverses then in a straight line the vacuum chamber to hit the wafer on the other side and form a thin film. To reach a uniform distribution and cover only the lateral, but not the vertical surfaces on the target (to avoid fences), the performance of the vacuum and the distance between the target and the deposition material are essential. The larger the distance between source and target and the better the vacuum, the less collisions between the evaporated molecules occur and the straighter/more vertical the molecules stick to the target. The used CMi machine, Alliance-Concept EVA760, disposes of a cryogenic pump, which ensures the required vacuum and has a variable distance between the source and the rotating dome, which was chosen to be at the maximal configuration (450mm) (CMi, 2018). The heating of the source happens either by an electron beam such as in the EVA760 or by a thermal filament. The e-beam is based on a tiny hot filament that boils off electrons, which are then magnetically guided towards the source and sputter away the platinum and chromium molecules. Even though the platinum layers were supposed to be 20nm thick, the deposited layers finally consisted of 2nm chromium and 18nm platinum. The reason for this split up is the improved adhesion of Cr on Si/ SiO₂ surfaces compared to Pt (Guarnieri & al, 2017). The deposited layer thickness is instantly measured through the frequency change of the inbuilt quartz crystal (Hardy, 2013).

2.4 Atomic Layer Deposition (ALD)

Although ALD is also a thin film deposition process like thermal evaporation it has two crucial differences. First, based on the principle of monolayer deposition, its thickness control is more accurate and secondly, the atoms do attach on all sides of the substrate and do not only come from one direction. The process consists of four steps, which are consecutively repeated until the desired thickness is achieved (figure 8). In the beginning the 1st precursor gets pulsed into the reaction chamber and adheres by chemisorption

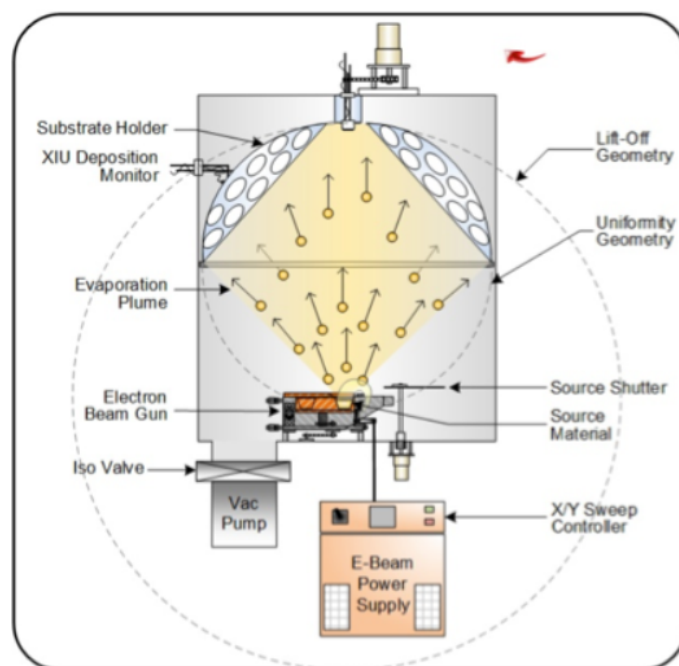


Figure 7: Schematic representation an E-Beam evaporator.
(Hardy, 2013)

to the surface of the wafer. All unnecessary additional atoms stay unbounded and are in step two blown out of the chamber by an inert gas (N_2). The reactor is then floated with the second precursor, which bonds only to the first precursor and forms the desired monolayer and a byproduct. In the last stage, the reaction chamber is again purged with the inert gas to get rid of precursor 2 excess and make it ready to start all over again. The 500 cycles required to deposit 50nm of HfO_2 were done in the ALD Beneq TFS200 at 200°C and TEMAHf was used as precursor 1, respectively H_2O as precursor 2 (CMi, 2020).

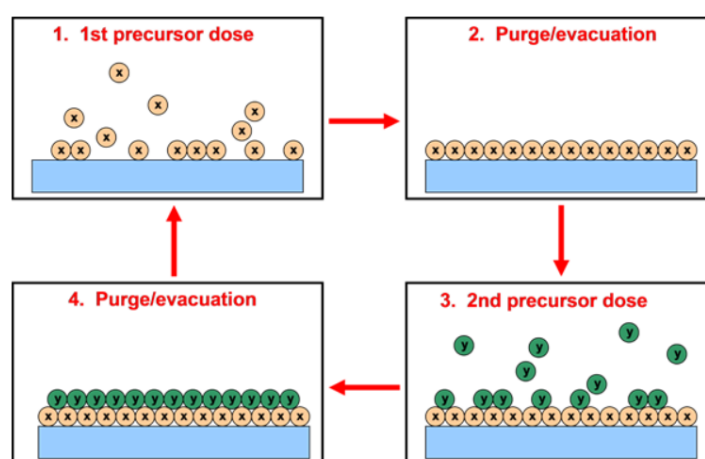


Figure 8: Schematic representation of an atomic layer deposition cycle
(Lesker, 2016)

2.5 Lift-Off

Contrariwise to etching, which attacks directly a material, the deposited material in lift-off gets taken off via the removal of the underlying photoresist layer. As it can be noted in figure 9 a photoresist pattern is deposited on a substrate on which another layer is deposited (for instance by thermal evaporation or ALD). While the photoresist mask, and consequently the material on top of it, are removed by a chemical bath, the directly on the substrate deposited material is not attacked. The whole process took place at the Plade Solvent bench in zone 01, where the LOR5A and AZ1512 coated wafers were kept in a Remover 1165 bath for 24 hours (CMI, 2020). Thanks to the double development explained in subsection 2.1 and the achieved results in subsection 2.7, no ultrasonic bath was needed to break fences.

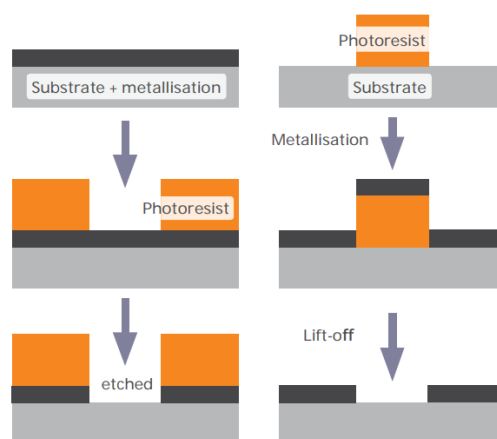


Figure 9: Schematic representation of etching vs. lift-off.
(MicroChemicals, 2022)

2.6 Stress Measurement

The FLX 2320-S from Toho Technology allows to measure the internal stress of thin films and substrates. This is of interest as most depositions happen at a relatively high temperature, whereas the application's environment is at room temperature. Having a large difference in the thermal expansion coefficient could consequently influence the bonding, respectively the crystalline structure of HfO₂ on the substrate/ platinum. The machine itself scans the wafer with a laser, which is, depending on the surface radii, with a specific angle reflected to a detector. Knowing the new angle of reflection (i.e. radius of curvature) after each film deposition and the thickness of the layers, the system can automatically calculate the internal stress of the films. Based on the measurements from the LR wafer in figure 12 and the other two wafers in appendix B, one can conclude that even if platinum (linear expansion coefficient: $9 \times 10^{-6} m/(m^{\circ}C)$) has a two to three times a higher linear thermal expansion coefficient than *Si* ($3 - 5 \times 10^{-6} m/(m^{\circ}C)$) (ET, 2003), it can not sustainably affect the bending of the wafer due to its thinness. On the other hand one can see that the deposited HfO₂, even though only 50nm thin, manages to bend the wafers around 3 more micrometers and multiplies the internal stress almost three times. Given the fact that the wafer is bent towards the upper side, the HfO₂ is exposed to tensile stress and has a larger thermal expansion coefficient than Si.

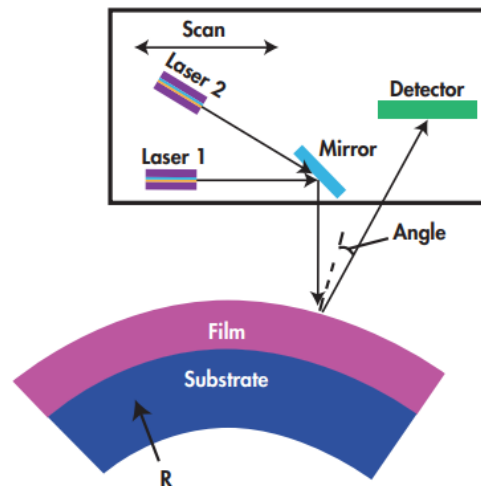


Figure 10: Schematic representation of stress measurement.
(Toho, 2019)

2.7 Fence Height Measurement (sideproject)

Such as explained in subchapters 2.1 and 2.3 the main issue of thermal evaporation is fence building at lateral walls. This means that the sputtered molecules do not only attach on the horizontal (desired) surfaces, but do also accumulate on the vertical walls. Like aforementioned, this can be caused by too many collisions between the molecules (vacuum not strong enough) or by a too short distance between the source and the substrate, which then provokes lateral moving molecules. The taken approach to use two photoresists and to do double development proved itself to be reliable, as it can be seen in figure 11. The fences are clearly below 50nm, which would cause a short circuit between the two Cr/ Pt layers. The measurement was done with the Bruker Dektak XT surface profiler, which uses a tiny tip with a torque measuring feedback system to glide over the surface and reconstruct the topology (Nanoscience, 2022) (Bruker, -).

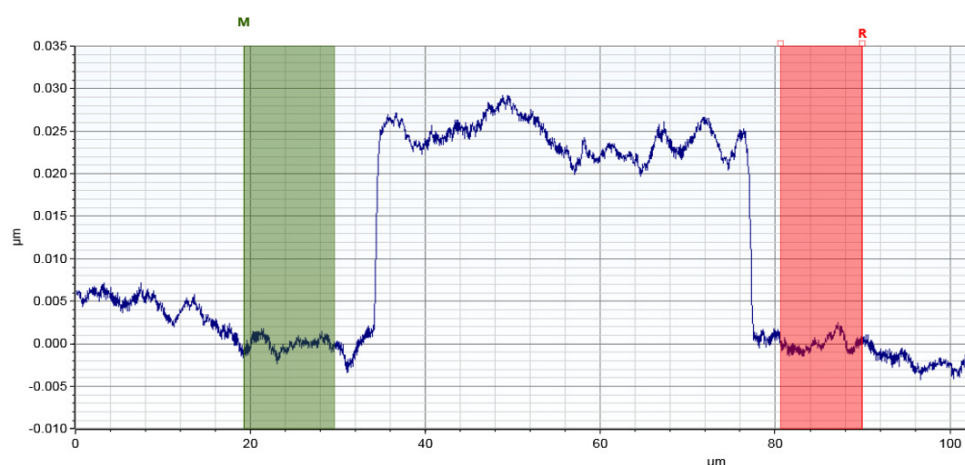


Figure 11: Surface topology and (non-existing) fences.

2.8 Thickness Measurement

One way to check the distribution uniformity and the thickness of a deposited material is to use a spectroscopic reflectometer. The machine, for instance the F-54, which tests the thickness at 41 spots, does send light at a specific wavelength to the wafer, which is then partly reflected at each translucent layer and captured by a detector. By taking into account the refractive index n and the extinction coefficient of the material, as well as the phase difference between the sent and received light, the system can determine the thickness of the layers. The results achieved for the LR wafer can be seen in figure 13, whereas the results for the other 2 wafers can be found in appendix C. At first sight, the results don't seem very promising as on one hand the uniformity throughout the measurement is not given and on the other hand the mean thicknesses have enormous deviations from the desired $20nm$, resp $50nm$. However, the lower range of the machine is $20nm$, its accuracy $2nm$ and when comparing measurements after 2 or 3 depositions, one can conclude that the machine's laser has difficulties to penetrate several layers. Hence, considering only the top layer of each measurement and taking into account the reflectometer's limits, the distribution uniformity and thickness of each wafer can be classified as satisfying.

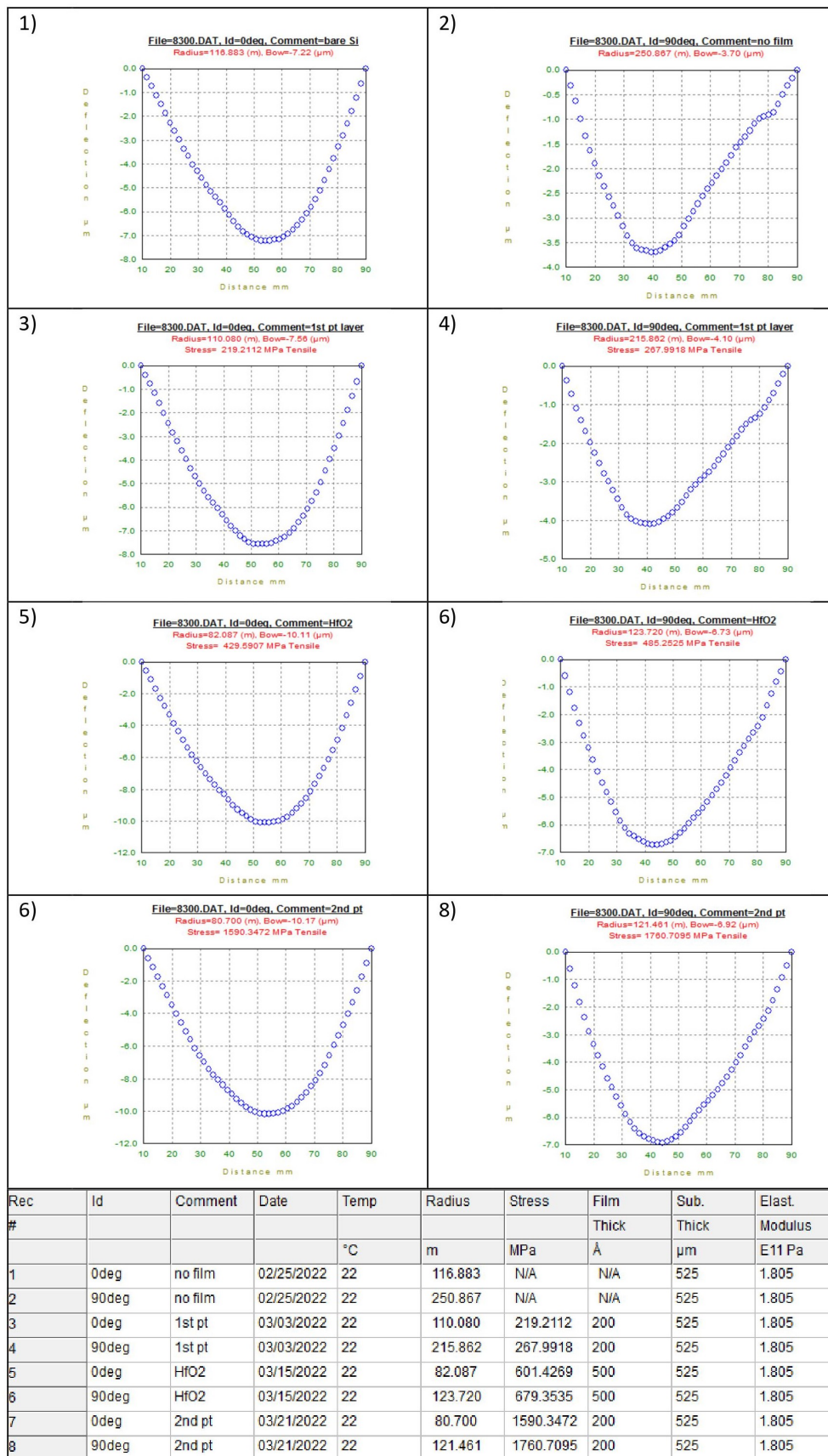


Figure 12: LR wafer: Stress and curvature measurements over 2 directions.

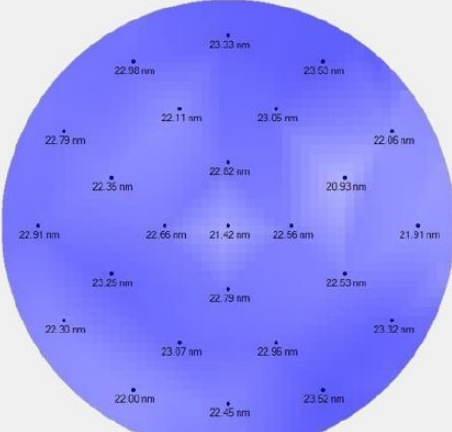
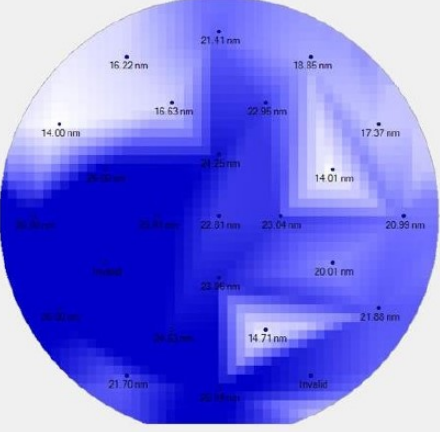
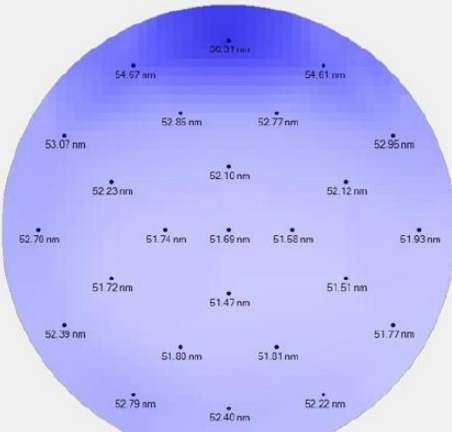
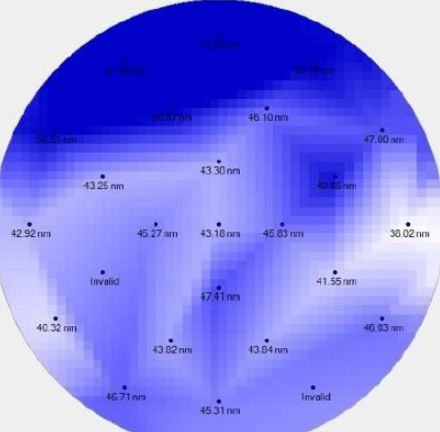

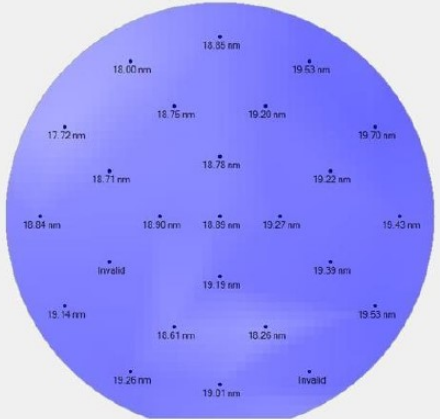
LR Wafer	Thickness measurement after 2 deposited layers	Thickness measurement after 3 deposited layers
1 st Cr/ Pt layer		
HfO ₂ layer		
2 nd Cr/Pt layer		
Averages	<p>HfO₂ = 51.69 nm Pt = 21.42 nm Goodness of fit = 0.99907</p>	<p>Pt = 18.89 nm HfO₂ = 43.18 nm Pt = 22.81 nm Goodness of fit = 0.99834</p>

Figure 13: LR Wafer: Thickness measurements after 2 (left) and 3 (right) deposits.

3 HfO₂ Crystallization

After having discussed the microfabrication of the Pt/ HfO₂ samples in the previous chapter, this section aims to deal with the HfO₂ crystallization. A brief summary of crystallization and its importance for HfO₂ thin films can be found in subsection 3.1, followed by an introduction into annealing (3.2) and X-ray diffractometry (3.3). The chapter then presents the results obtained on the three different substrates with the 2θ measurements (3.4) and finally discusses the detected crystallization phases in subsection 3.5.

3.1 Crystallinity

Crystallinity describes the molecule's degree of structural order (Cheng & al, 2017) and can influence a materials' parameters. HfO₂ thin films can either be found in an amorphous state (e.g. after ALD) or in a crystal state (e.g. after annealing). The latter can be divided into three different categories, namely monoclinic, tetragonal or orthorhombic. HfO₂ can either be found in a single phase such as in figure 14 or in a multiphase (i.e several phases coexist at the same time) state. Depending on the crystal phase, the material's parameters such as refractive index, optical gap, dielectric constant (Zhang & al, 2019) or the polarity change. Having a non symmetric crystal lattice, might induce a polarization in the material and lead to a piezoelectric manner. It is therefore of great interest to know the crystal's lattice and its associated behavior.

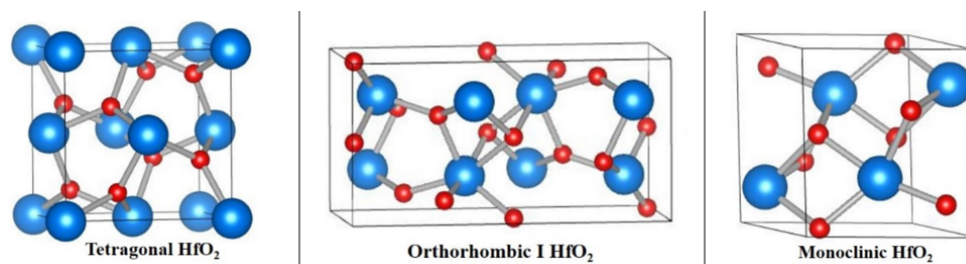


Figure 14: HfO₂ crystal structures, from left to right: Tetragonal, Orthorhombic I, Monoclinic. (Vargas, 2014)

3.2 Annealing

Annealing is a process to alter the physical structure of a material by heating it above its recrystallization temperature, hold it there for a determined amount of time and cool it down at a specific rate (TWI, 2022a). Above this recrystallization point, which is probably atom mass dependant (Hsain & al, 2020) and which is around 500°C for HfO₂ (Zhang & al, 2019), the atoms and molecules start to reorganize/ diffuse in order to form a single crystal phase (with HfO₂ monoclinic, tetragonal or orthorhombic) or a multiphase (composition of the three). The annealing was done with the Neytech Qex Furnace in CMi, which offers a controlled heating rate up to 1200°C with nitrogen gas flow. Unfortunately, the machine does not possess an enforced cooling option and consequently samples were only cooled down by ambient air or even slower. To have enough samples, the 3 wafers were diced into 1.5 x 1.5cm large chips before the annealing.

3.3 X-Ray Diffractometry

An X-ray diffractometer illuminates a crystal lattice with a (in theory) focused monochromatic X-ray beam to make the atoms scatter the electromagnetic waves. Although most of the generated waves cancel each other out by destructive interference, some waves behave in a constructive way and form a diffraction pattern based on Bragg's law. The spots appearing on the detector (i.e. reflections), respectively their angles of origin and intensities determine the chemical structure and therefore the corresponding material (TWI, 2022b). To analyse the chips, the Bruker D8 Discovery with a 0.02mm large nickel filter (to avoid saturation of the detector) from the Institute of Chemical Sciences and Engineering at EPFL was used (Bruker, 2022).

3.4 Results

To identify the appearing peaks on the three different substrates, LR (figure 15), HR and LR with SiO₂ layer (both appendix D), the ICSD (FIZ Karlsruhe, -) and the *Materials Project* database (Various, -) were used. Both databases are open web-based and provide material analysis from diverse research projects, which are not necessarily certified, but can be verified by comparing different sources. The samples were heated to the corresponding number in the legend (in °C) at a heating rate of 20°C/min, except the ones with *2x heating rate*, which had a heating rate of 40°C/min. They were then kept for 15min at this temperature and subsequently cooled down, either by keeping them in the closed bell (cooling time around 2h, *long*) or by cooling them with an open bell at ambient air (cooling time around 1h, *short*). The peaks appearing very close together (for instance at Si (200)) can be considered as one reflection as they are produced by the XRD's non-monochromatic light emission, which is composed of two spectral lines ($k\alpha_1$ and $k\alpha_2$). All the identified peaks on figure 15 and their corresponding materials are listed hereby:

- **Si:** Silicon peaks have been found at 69.8° (hkl=400), at 37.8° (200/101) and at 33.0° (200). The Si (200) is called *forbidden reflection* and does only appear under specific circumstances (Zaumseil, 2015), which are not closer investigated in this work.
- **Pt:** Platinum consists normally of a strong reflection at 40.0° (111) and another one at around 45° (200), which can be well detected.
- **HfO₂:** Depending on the crystal phase of the hafnium oxide, the XRD analysis shows different 2θ reflections, which are either marked by *m* for monoclinic or by *t* for tetragonal. The peaks at 30.1° (101), 34.9° (002), 35.6° (110), 38° (101), 50.8° (112/200) and 60.3° (211) do belong to the tetragonal phase, whereas peaks 32.1° (111) and 54.4° (202) can be associated with the monoclinic phase.
- **SiO₂:** Although the reflection at 42.8° cannot be explained by silicon, platinum or hafnium oxide, SiO₂ (220) does have a peak at this location.

Even though a search algorithm on the open access database *Crystallography Open Database* has been ran for the reflection at 29.2°, no match for this peak has been found. Moreover, it is noteworthy that almost none of the HfO₂ reflections appear on the HR and LR with SiO₂ wafer (appendix: D). The absence of these HfO₂ reflections on the HR and Si with SiO₂ wafer and the appearance of the tetragonal and monoclinic peaks on the LR wafer are discussed in detail in the following chapter.

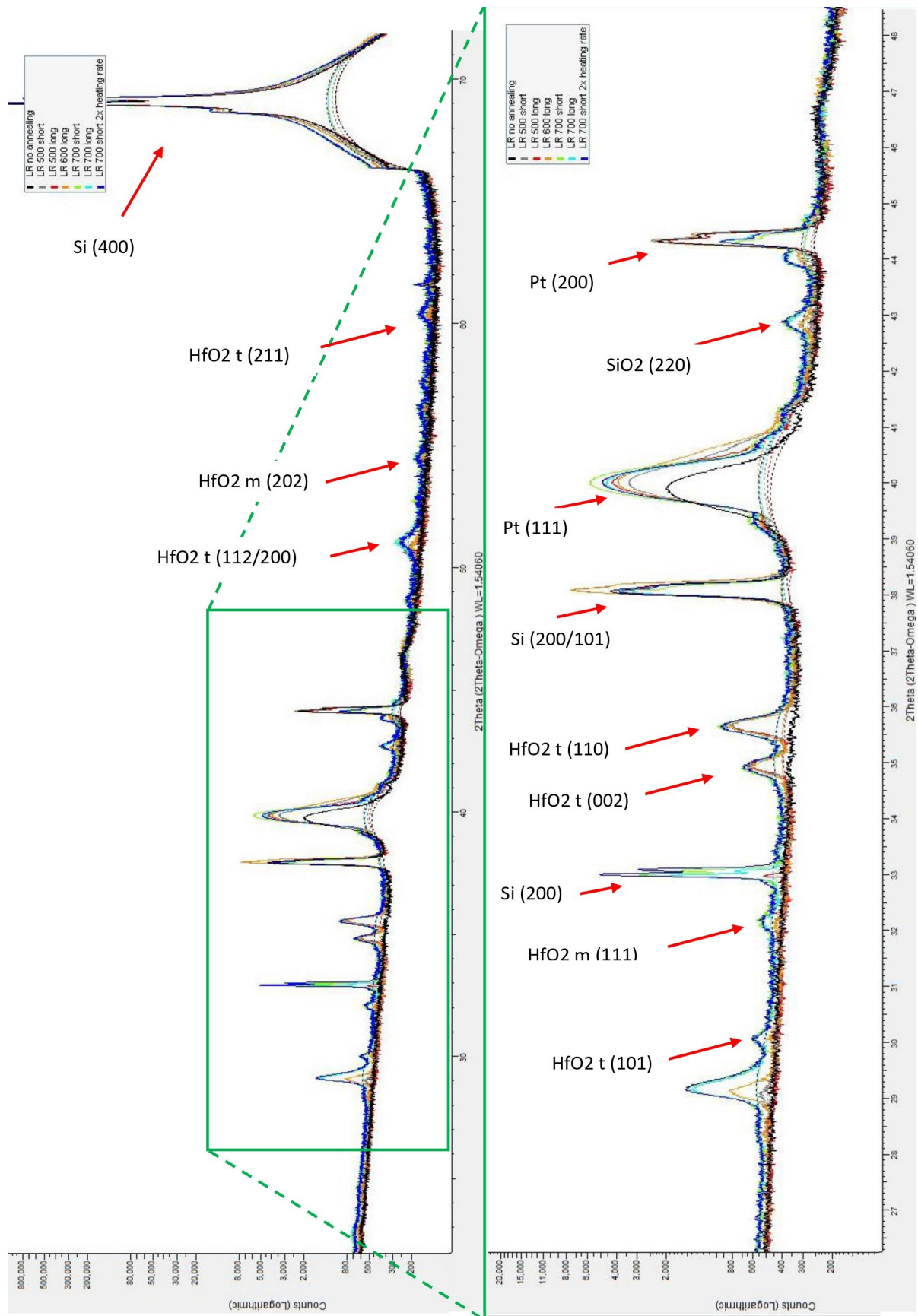


Figure 15: LR wafer: 2θ measurements after annealing.

3.5 Discussion

Mainly based on the achieved results with the LR wafer, but also on the other wafers, several conclusions can be drawn:

- The atomic layer deposition of HfO₂, which takes place at around 200°C deposits the material in an amorphous state. Heating the material only slightly above the recrystallization temperature to 500°C alters the amorphous structure into a mainly tetragonal crystal lattice. Considering the work from (Zhang & al, 2019) and the inaccuracy of the X-Ray diffractometer, additional phases cannot be excluded.
- No difference can be identified between cooling down at room temperature and a slowed down cooling in the heating capsule. Enforced cooling, such as done with metals could be worth a trial to investigate the behavior of the structures. However, H. Alex Hsain, author of papers in the HfO₂ thin film domain such as (Hsain & al, 2020), predicts that this doesn't lead to monoclinic structures.
- Probably most interesting for further studies is the fact that the monoclinic peaks at 32.1° and 54.4° do only appear for 700°C and not for cooler temperatures. Considering the still existing tetragonal phase, it needs to be explored if the material stays in a multiphase condition or if the monoclinic phase replaces the tetragonal one for hotter temperatures. Nevertheless, it can be concluded that the annealing temperature must be at least somewhere around 700°C to start forming monoclinic lattices in the material.
- Doubling the heating rate from 20°C/min to 40°C/min has given exactly the same reflections for the 700°C trial. Hence, it can be assumed that the heating rate doesn't play a significant role in the structure deforming.
- This work has not analysed the time being at maximum temperature, which means that all samples were kept on top for 15min. However, the work from (Ho & al, 2002) has examined the corresponding behavior of thin film HfO₂ and shown that the duration on top does neither matter.
- The reason why only two tetragonal reflections on the HR and LR with SiO₂ wafers have been detected after annealing is difficult to evaluate. One explanation could be that these substrates induce a different HfO₂ deposition order after ALD. (Ho & al, 2002) have shown that on some substrates, HfO₂ is in an amorphous condition with a strong order on a subnanometer scale, rather than just in simple amorphous condition. However, they have also shown that this deposition behaves in a known way when doing annealing. Considering therefore this work and the results achieved in this project, further annealing with higher temperatures should be done to see the happening.

4 Conclusion

Main goal of this project was to collect more knowledge in the field of microfabrication and HfO₂ annealing/ crystallization.

On one hand, based on the process flow from *Ph.D. D. Moreno* and *A. Elisei* several microfabrication steps to manufacture piezoelectric HfO₂ resonators in CMi could be refined and/or verified. Taking the parameters given in the process flow in appendix A and in chapter 2, it is now possible to pattern, deposit and remove materials in a way, such that a uniform distribution is achieved and no fences are produced. Moreover, knowing the internal stress induced by platinum or hafnium oxide layers on Si wafers, further designs can consider these facts.

On the other hand, even though no pure monoclinic HfO₂ structure could have been produced by annealing, several conclusions on the development of HfO₂ crystal lattices were established. It can be said, that neither the heating rate, nor the cooling rate or the time being at maximum temperature play a significant role for the desired monoclinic phase. Nonetheless, it can be assumed that the transformation from the amorphous HfO₂ structure after ALD into a tetragonal, respectively monoclinic crystal phase depends on the maximum temperature. Especially latter mentioned is only formed at temperatures above around 700°C on normal Si 0.1 – 100Ω-cm substrates.

References

- Bruker. (-). *Dektak xtl*. <https://www.bruker.com/en/products-and-solutions/test-and-measurement/stylus-profilometers/dektak-xtl.html>. (Accessed: 2022-06-01)
- Bruker. (2022). *D8 discover family*. [https://www.bruker.com/en/products-and-solutions/diffractometers-and-scattering-systems/x-ray-diffractometers/d8-discover-family.html?sc_cid=SEMB&campaign=D8_Discover_NA/Europe\(XRD\)&source=google&medium=cpc&keyword=&device=c&gclid=EAIaIQobChMI9ayk9uaM-AIVSI9oCR3MNQ1UEAAAYASAAEgKN4vD_BwE](https://www.bruker.com/en/products-and-solutions/diffractometers-and-scattering-systems/x-ray-diffractometers/d8-discover-family.html?sc_cid=SEMB&campaign=D8_Discover_NA/Europe(XRD)&source=google&medium=cpc&keyword=&device=c&gclid=EAIaIQobChMI9ayk9uaM-AIVSI9oCR3MNQ1UEAAAYASAAEgKN4vD_BwE). (Accessed: 2022-06-02)
- Cheng, S. Z., & al. (2017). *Introduction to the physical, mechanical, and thermal properties of plastics and elastomers*. <https://www.sciencedirect.com/topics/chemistry/crystallinity>. (Accessed: 2022-06-02)
- Cirelli, & al. (2001). *Optical lithography*. <https://www.sciencedirect.com/topics/materials-science/optical-lithography#:~:text=Photolithography%20is%20a%20patterning%20process,access%20to%20an%20underlying%20substrate>. (Accessed: 2022-05-26)
- CMi. (2018). *Alliance-concept eva 760*. <https://www.epfl.ch/research/facilities/cmi/equipment/thin-films/alliance-concept-eva-760/>. (Accessed: 2022-05-27)
- CMi. (2019). *Tepla gigabatch*. <https://www.epfl.ch/research/facilities/cmi/equipment/etching/tepla-gigabatch/>. (Accessed: 2022-05-27)
- CMi. (2020). *Ald beneq tfs200*. <https://www.epfl.ch/research/facilities/cmi/equipment/thin-films/atomic-layer-deposition-beneq-tfs200-ald-1/>. (Accessed: 2022-05-27)
- CMi. (2020). *Plade solvent, lift-off*. <https://www.epfl.ch/research/facilities/cmi/equipment/photolithography/plade-solvent-wet-bench-for-lift-off-and-su-8-development/plade-solvent-lift-off-manual/>. (Accessed: 2022-06-02)
- CMi: Racine G.-A. (2020). *Evg150*. <https://www.epfl.ch/research/facilities/cmi/equipment/photolithography/evg-150-automatic-resist-processing-cluster/>. (Accessed: 2022-05-26)
- ET, T. E. T. (2003). *Thermal expansion - linear expansion coefficients*. https://www.engineeringtoolbox.com/linear-expansion-coefficients-d_95.html. (Accessed: 2022-06-02)
- FIZ Karlsruhe. (-). *Icsd*. <https://icsd.fiz-karlsruhe.de/index.xhtml;jsessionid=9C989F0DE8CCE4682381BC284357BDE4>. (Accessed: 2022-06-02)
- Guarnieri, V., & al. (2017). *Platinum metallization for mems application*. <https://pubmed.ncbi.nlm.nih.gov/24743057/>. (Accessed: 2022-05-27)
- Hardy, N. (2013). *What is thin film deposition by thermal evaporation?* <http://www.semicore.com/news/71-thin-film-deposition-thermal-evaporation>. (Accessed: 2022-05-27)
- Heidelberg. (2022). *Maskless laser lithography*. <https://heidelberg-instruments.com/key-features/maskless-laser-lithography/>. (Accessed: 2022-05-27)
- Ho, M.-Y., & al. (2002). *Morphology and crystallization kinetics in hfo2 thin films grown by atomic layer deposition*. <https://aip.scitation.org/doi/pdf/10.1063/1.1534381>. (Accessed: 2022-06-02)

- Hsain, H. A., & al. (2020). *Compositional dependence of crystallization temperatures and phase evolution in hafnia/zirconia (hfxzr1x)o₂ thin films*. <https://aip.scitation.org/doi/10.1063/5.0002835>. (Accessed: 2022-06-02)
- Lesker, K. J. (2016). *Herausforderungen für nicht-ideale atomare schichtdepositionsprozesse und -systeme*. <https://de.lesker.com/blog/challenges-for-non-ideal-atomic-layer-deposition-processes-systems>. (Accessed: 2022-05-27)
- MicroChemicals. (2022). *Lift-off*. https://www.microchemicals.com/technical_information/lift_off_photoresist.pdf. (Accessed: 2022-06-02)
- Nanoscience. (2022). *Stylus profilometry*. <https://www.nanoscience.com/techniques/optical-profilometry/stylus/>. (Accessed: 2022-06-01)
- PIC. (-). *Photoresist ashing, stripping, and descum. organic contamination removal for silicon wafer*. https://piescientific.com/application_pages/applications_silicon_wafer/. (Accessed: 2022-05-27)
- Samco. (-). *Plasma ashing of photoresist*. <https://www.samcointl.com/featured-solutions/photoresist-removal/>. (Accessed: 2022-05-27)
- Toho. (2019). *Flx 2320-s*. https://tohototechnology.com/wp-content/uploads/2019/09/Toho_FLX2320S_D1.pdf. (Accessed: 2022-06-01)
- TWI. (2022a). *What is annealing? a complete process guide*. <https://www.twi-global.com/technical-knowledge/faqs/what-is-annealing>. (Accessed: 2022-06-01)
- TWI. (2022b). *What is x-ray diffraction analysis (xrd) and how does it work?* <https://www.twi-global.com/technical-knowledge/faqs/x-ray-diffraction>. (Accessed: 2022-06-02)
- Vargas, M. (2014). *Nanometric structure-property relationship in hafnium oxide thin films made by sputterdeposition*. https://scholarworks.utep.edu/cgi/viewcontent.cgi?article=2368&context=open_etd. (Accessed: 2022-06-10)
- Various. (-). *Materialsproject*. <https://materialsproject.org/>. (Accessed: 2022-06-02)
- Zaumseil, P. (2015). *igh-resolution characterization of the forbidden si 200 and si 222 reflections*. <https://www.ncbi.nlm.nih.gov/pmc/articles/PMC4379439/#bb7>. (Accessed: 2022-06-02)
- Zhang, X.-Y., & al. (2019). *Temperature-dependent hfo₂/si interface structural evolution and its mechanism*. <https://nanoscalereslett.springeropen.com/track/pdf/10.1186/s11671-019-2915-0.pdf>. (Accessed: 2022-06-02)

A Process Flow

Lab : Advanced NEMS LAB
 Operator Name : **Andrea Bruder**
 Supervisor Name : Daniel Moreno Garcia
 Date of committee :

Téléphone : +41 79 567 32 65
 Office : MED 2 2726 (Supervisor)
 E-mail : andrea.bruder@epfl.ch

CMi EPFL Center of
 MicroNanoTechnology

Semestral Project Master Project Thesis Other

HfO₂ NEMS

Description

Goal of this project is to fabricate crystalline chips to investigate the annealing process of HfO₂. The project can be expanded into fabricating nanoactuators (sideproject). Please note that the crossed out process steps belong to the sideproject and haven't been done in this semester project.









Technologies used <i>!! remove non-used !!</i>			
Main Project: Descume, Thermal Evaporation, ALD, Metrology, Dicing, Annealing Sideproject: Photolithography, Lift-Off, Dry Etching, Wet Etching, SEM, AFM, Chip-level processing			
Photolithography masks			
Mask #	Critical Dimension	Critical Alignment	Remarks
1	10 um	First Mask	Bottom electrode liftoff
2	10 um	1 um	Top electrode definition
3	20 um	2 um	Electrode pad liftoff
4	2 um	1 um	Resonator release
Substrate Type			
Si <100>, Ø100mm, Thickness 525 um, 0.1-100 Ohm.cm Si <100>, Ø100mm, Thickness 525 um, >10'000 Ohm.cm Si <100>, Ø100mm, Thickness 525 um, 0.1-100 Ohm.cm with 2um SiO ₂ wet oxide			

Lab : Advanced NEMS LAB
 Operator Name : **Andrea Bruder**
 Supervisor Name : Daniel Moreno Garcia
 Date of committee :

Téléphone : +41 79 567 32 65
 Office : MED 2 2726 (Supervisor)
 E-mail : andrea.bruder@epfl.ch

CMi EPFL Center of
 MicroNanoTechnology

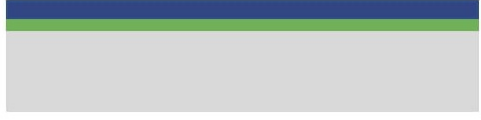
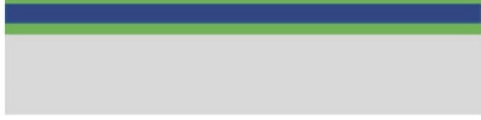


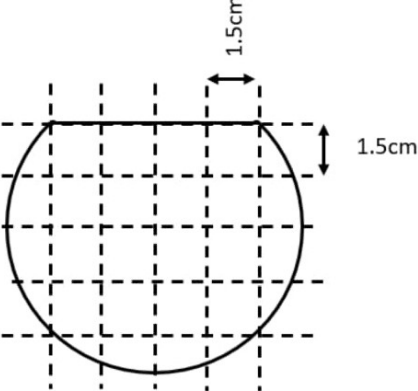
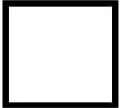
Process outline

Step	Process description	Cross-section after process	Key Parameters
01	<i>Stress Measurement</i> Toho		0 ° and 90 ° orientation
02	<i>Photolithography (sideproject)</i> EVG150 MLA150		PR: LOR5A (0.48um) and AZ1512 (1.1um) Std Dehydration Exposure: 55mJ/cm ² Laser Src : λ = 405nm Double Development
03	<i>Descum</i> TeplaGiGAbatch		Low Power (200W) Duration: 30s
04	<i>Evaporation</i> EVA760		2nm Cr and 18nm Pt 450mm distance between source and dome
05	<i>Stress Measurement</i> Toho		0 ° and 90 ° orientation
06	<i>Lift-Off (sideproject)</i> Remover 1165 Bath		Duration: 24h No US bath
07	<i>Fence Measurement (sideproject)</i> Bruker Dektak XT surface profiler		Range: 6.5um Stylus Force: 2mg Resolution: ~100 to 150um in 10-20sec
08	<i>ALD</i> Beneq TFS200		500 cycles HfO ₂ Reactor Temp: 200 °C Hot Source Temp: 80°C

Lab : Advanced NEMS LAB
 Operator Name : **Andrea Bruder**
 Supervisor Name : Daniel Moreno Garcia
 Date of committee :

Téléphone : +41 79 567 32 65
 Office : MED 2 2726 (Supervisor)
 E-mail : andrea.bruder@epfl.ch



<p>09</p>	<p><i>Stress Measurement</i> Toho</p>		<p>0 ° and 90 ° orientation</p>
<p>10</p>	<p><i>Evaporation</i> EVA760</p>		<p>2nm Cr and 18nm Pt 450mm distance between source and dome</p>
<p>11</p>	<p><i>Stress Measurement</i> Toho</p>		<p>0 ° and 90 ° orientation</p>
<p>12</p>	<p><i>Thickness Measurement</i> F54</p>		<p>Measurement done at 41 points</p>
<p>13</p>	<p><i>Dicing</i> Dicer Disco DAD321</p>		<p>1.5 x 1.5 cm pieces</p>
<p>14</p>	<p><i>Annealing</i> Neytech Qex Furnace</p>		<p>N2 gas flow For temperature and holding time refer to report</p>

Lab : Advanced NEMS LAB
 Operator Name : **Andrea Bruder**
 Supervisor Name : Daniel Moreno Garcia
 Date of committee :

Téléphone : +41 79 567 32 65
 Office : MED 2 2726 (Supervisor)
 E-mail : andrea.bruder@epfl.ch



This process steps belong uniquely to the fabrication of nanoactuators (sideproject) and were not done in this semester project. The process flow itself was designed by D. Moreno and A. Elisei and just copied herein for the sake of completeness.

15	<p><i>Photolithography</i> Machine: ACS200/MLA150 PR: AZ ECI3007 Thickness: 1 um</p>	
16	<p><i>Dry/Wet Etching</i> Machine: STS/HF Z2 Bench Material: Pt/HfO2 + Resist Strip</p> <p>Comment : wet etching of HfO2 has been proven effective in Kaitlin Howell's work.</p>	
17	<p><i>Photolithography</i> Machine: EVG150 + MLA150 PR: LOR+AZI512 Thickness: 0.48+1.1 um</p> <p>Includes: Descum O2 Plasma (10s). Machine: Tepla</p>	
18	<p><i>Evaporation and Liftoff</i> Machine: Lab 600/EVA 760 PR: Z1 bench solvent in permanent baths Material: Al Thicknesses: 500 nm</p>	
19	<p><i>Dicing of the samples</i> Machine: Dicer Disco DAD321 PR: Photoresist coating (AZ ECI) + dicing + Photoresist strip (remover 1165 Z2 UFT wet bench)</p>	

Lab : Advanced NEMS LAB
 Operator Name : **Andrea Bruder**
 Supervisor Name : Daniel Moreno Garcia
 Date of committee :

Téléphone : +41 79 567 32 65
 Office : MED 2 2726 (Supervisor)
 E-mail : andrea.bruder@epfl.ch



20	<i>Lithography</i> Machine: E-beam PR: CSAR Thickness: 600 nm	
21	<i>Dry Etching</i> Machine: STS Material: Pt/HfO ₂ +resist stripping	
22	<i>Cleaning residues</i> Etchant: HF (vapor) Material: HfO ₂	
23	<i>Dry Release</i> Etchant: XeF ₂ Material: Si	

Figure 16: Process flow (including sideproject).

B Stress Measurements

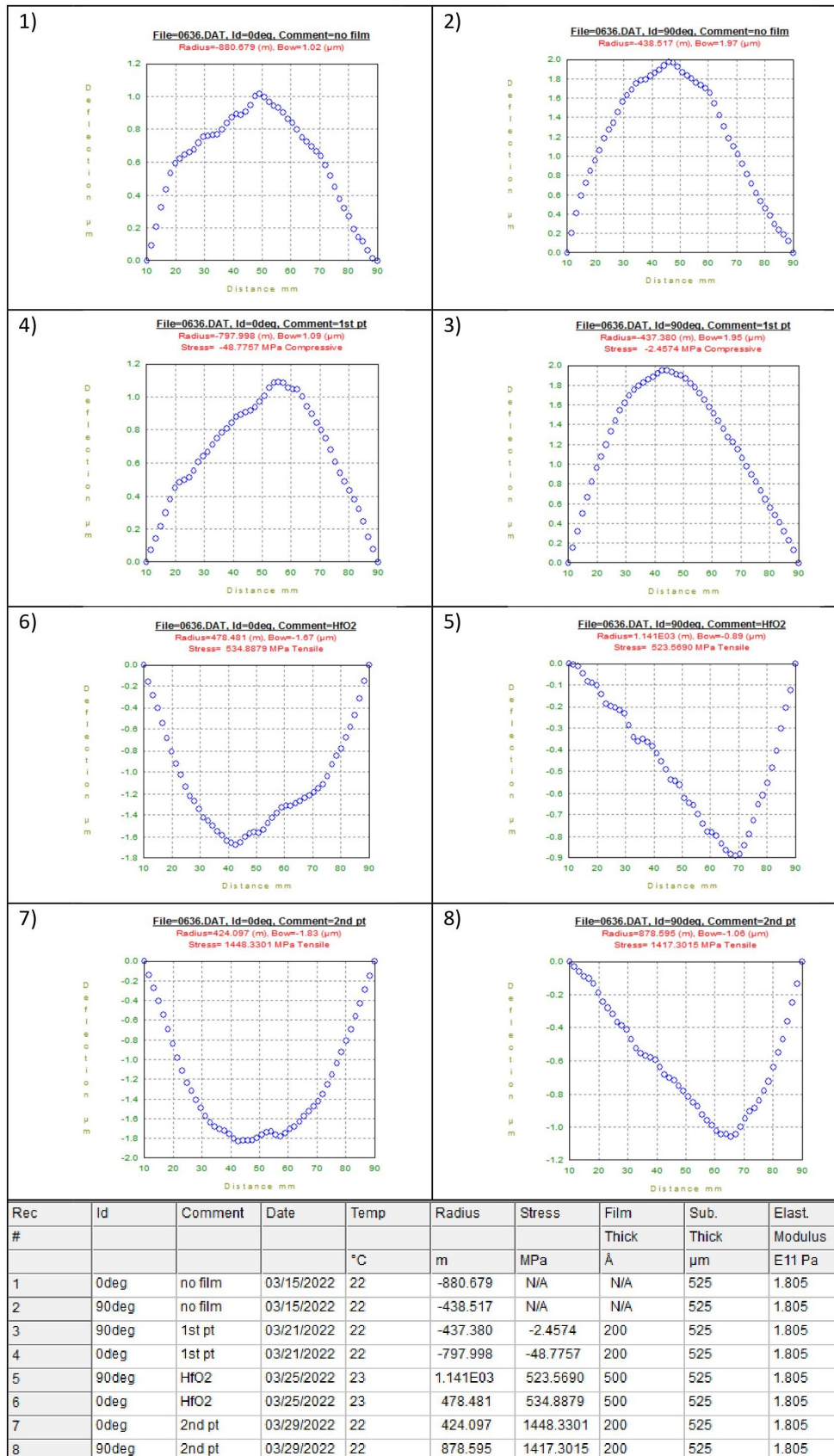


Figure 17: HR wafer: Stress and curvature measurements over 2 directions.

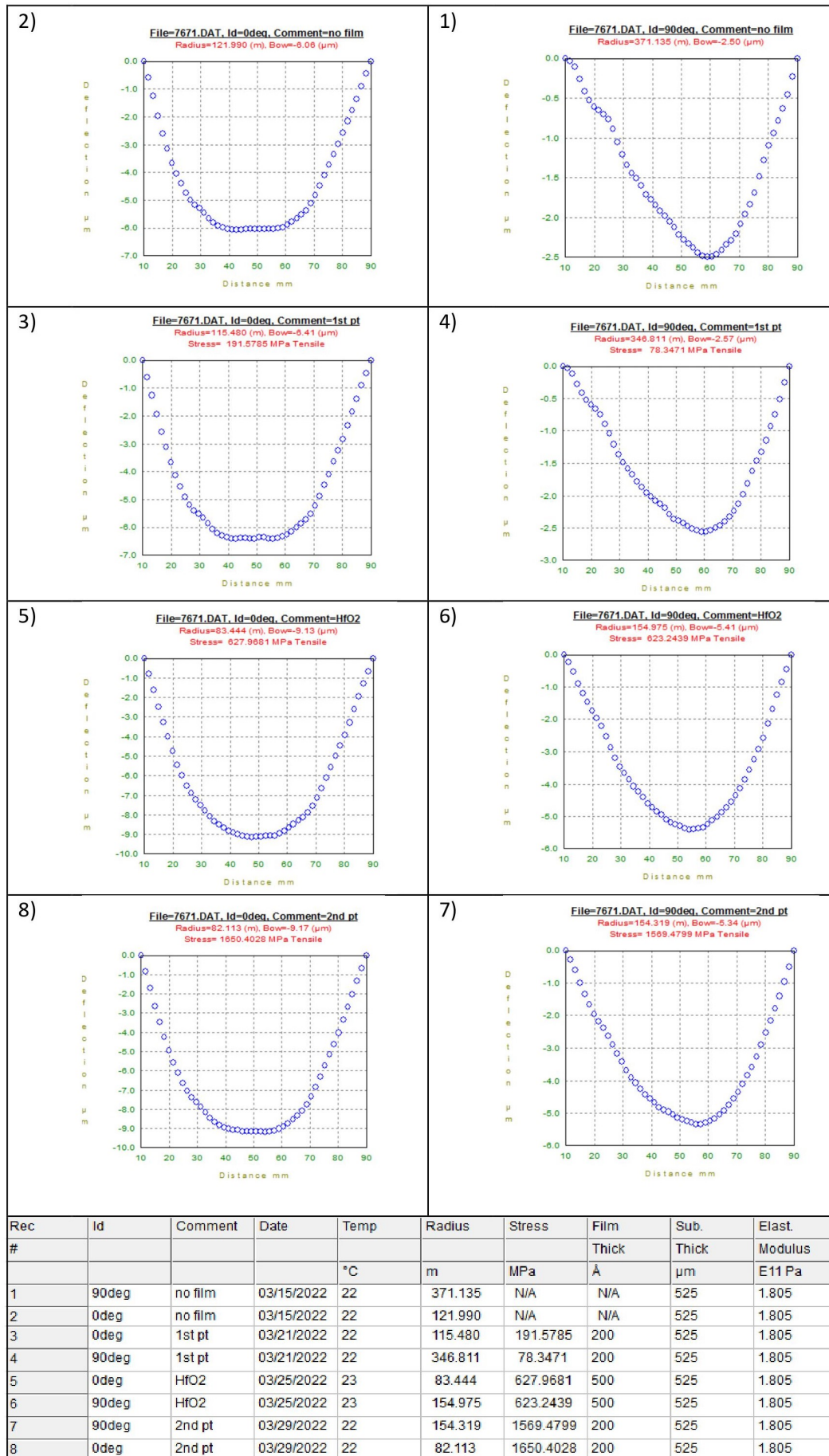


Figure 18: LR wafer with SiO₂: Stress and curvature measurements over 2 directions.

C Thickness Measurements

HR Wafer	Thickness measurement after 1 deposited layer	Thickness measurement after 2 deposited layers	Thickness measurement after 3 deposited layers
1 st Cr/ Pt layer			
HfO ₂ layer			
2 nd Cr/Pt layer			
Averages	<p>Pt = 19.99 nm Cr = 2.40 nm Goodness of fit = 0.98429</p>	<p>HfO₂ = 53.04 nm Pt = 22.91 nm Goodness of fit = 0.99885</p>	<p>Pt = 24.26 nm HfO₂ = 42.26 nm Pt = 25.80 nm Goodness of fit = 0.99596</p>

Figure 19: HR wafer: Thickness measurements after 1 (left), 2 (middle) and 3 (right) deposits.

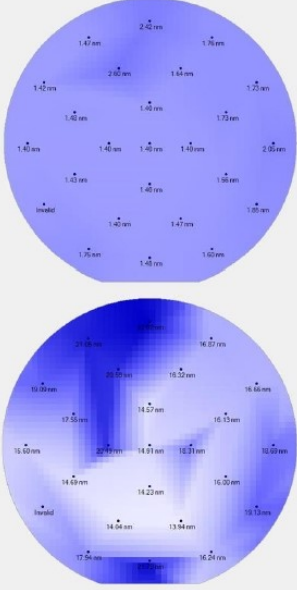
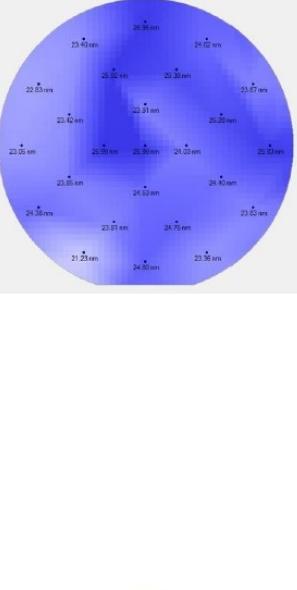
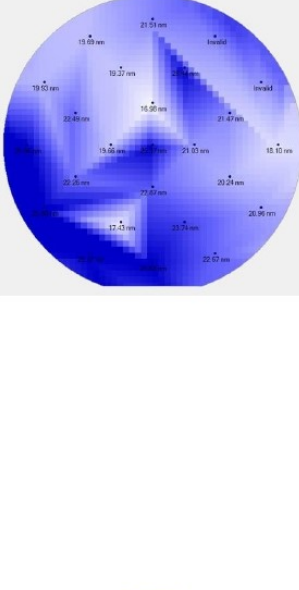
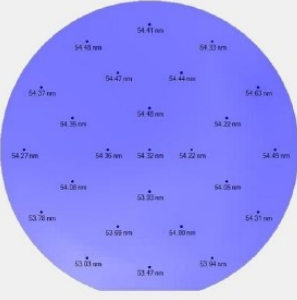
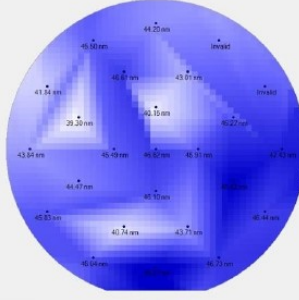
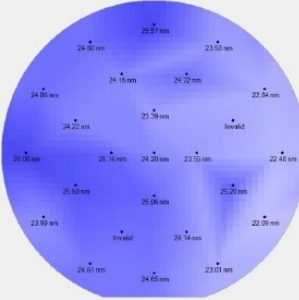
LR Wafer with SiO ₂ layer	Thickness measurement after 1 deposited layer	Thickness measurement after 2 deposited layers	Thickness measurement after 3 deposited layers
1 st Cr/ Pt layer			
HfO ₂ layer			
2 nd Cr/ Pt layer			
Averages	<p>Pt = 14.91 nm Cr = 1.40 nm Goodness of fit = 0.51825</p>	<p>HfO₂ = 54.32 nm Pt = 25.99 nm Goodness of fit = 0.89933</p>	<p>Pt = 24.20 nm HfO₂ = 45.75 nm Pt = 21.21 nm Goodness of fit = 0.99348</p>

Figure 20: LR with SiO₂ layer wafer: Thickness measurements after 1 (left), 2 (middle) and 3 (right) deposits.

D XRD 2θ Measurements

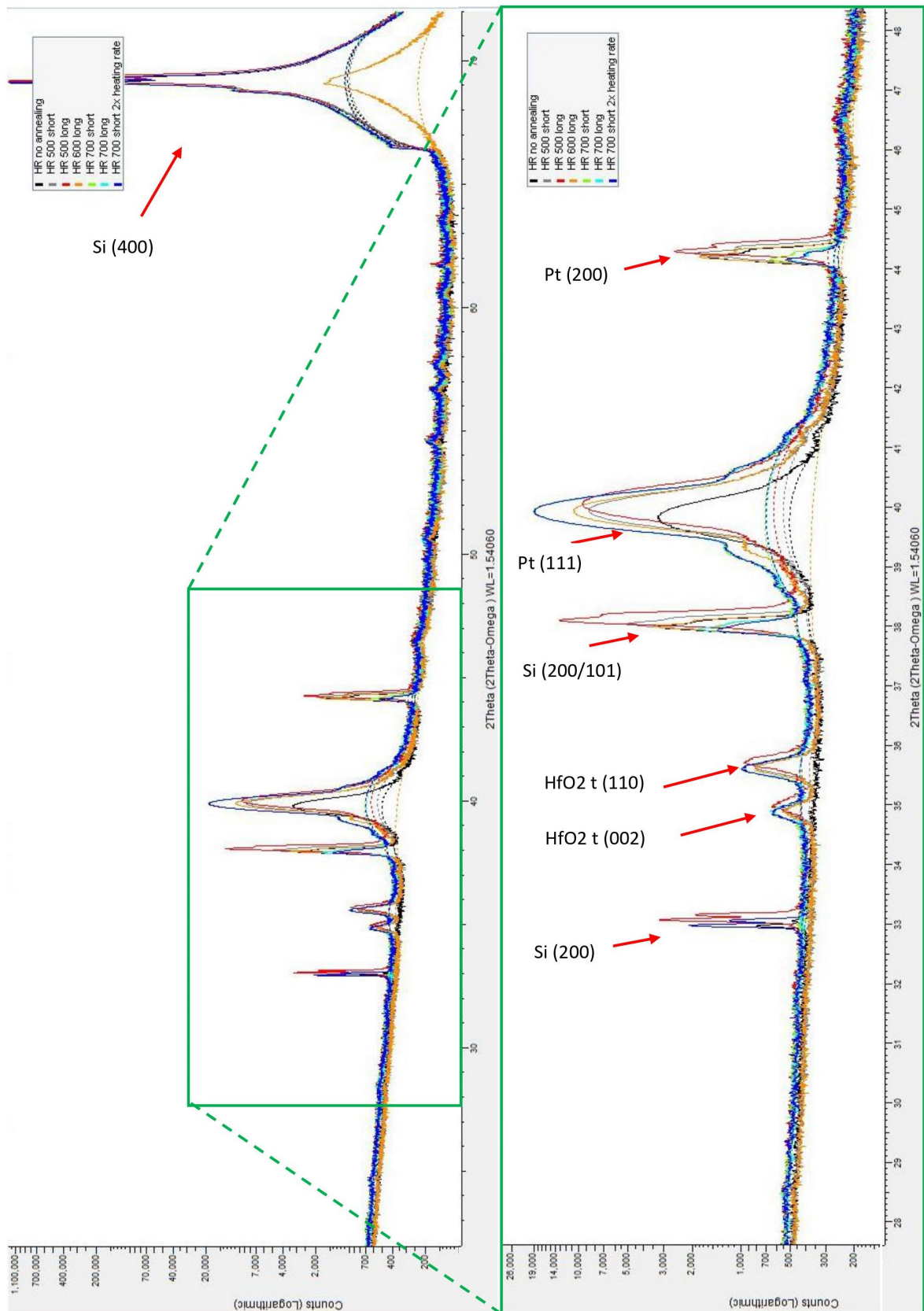


Figure 21: HR wafer (HR): 2θ measurements after annealing.

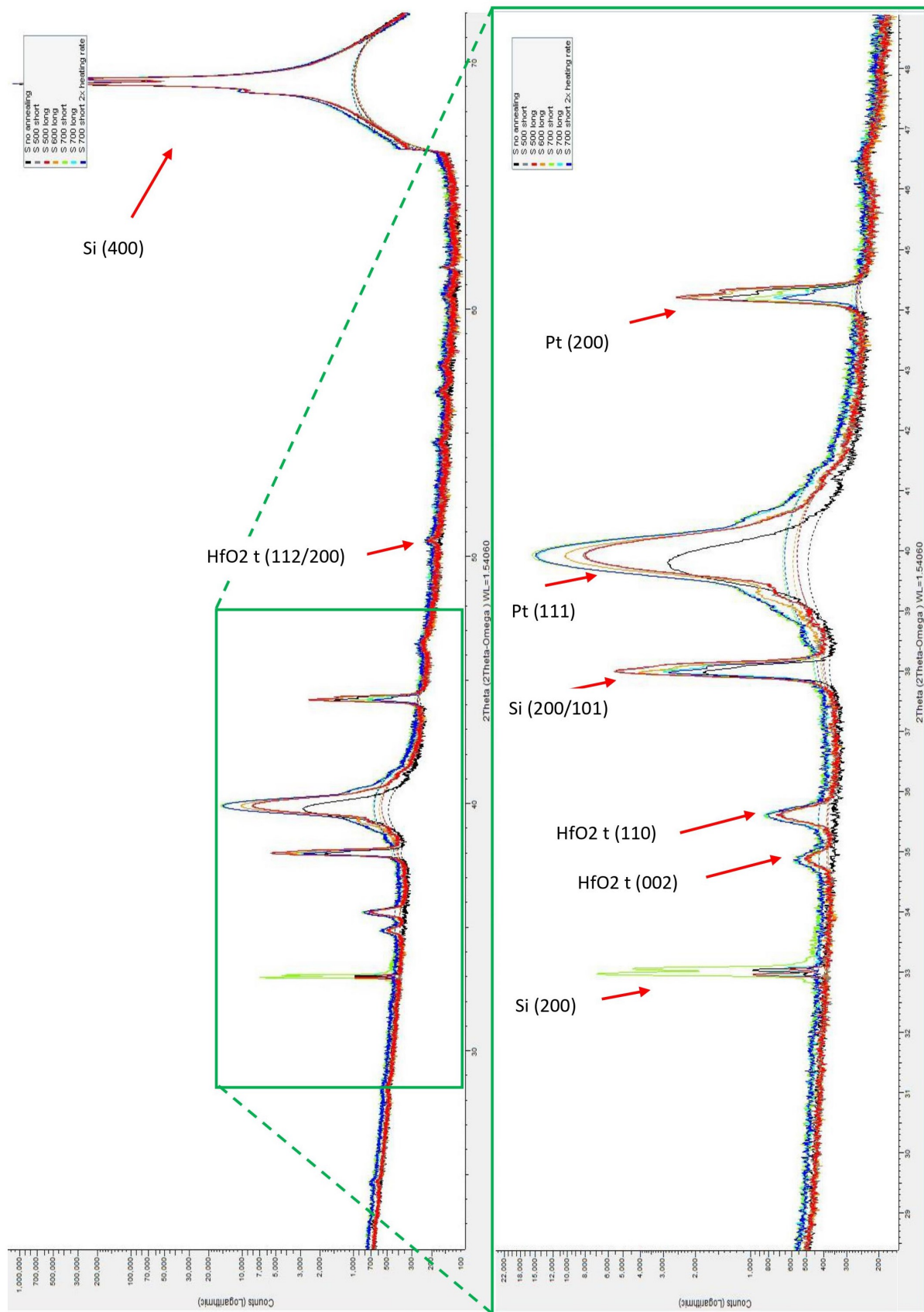


Figure 22: LR wafer with SiO₂ layer (S): 2θ measurements after annealing.